Indonesian Physical Review
Volume 08 Issue 02, May 2025
P-ISSN: 2615-1278, E-ISSN: 2614-7904

Analysis of Agricultural Soil Conditions 20 Years Post-Tsunami Using Resistivity and Soil pH Methods

Rahiel Adiannur[1*], Amsir[1*], Zakia Masrurah[1], Marwan[1], Mustapha Adejo Mohammed[2]
[1] *Geophysics Enginnering department, Faculty of Engineering, Syiah Kuala University, Indonesia*
[2] *Physics Department, Federal University of Lafia, PMB 146 Lafia, Nigeria*

Corresponding Authors E-mail: rahiel@mhs.usk.ac.id, amsir@usk.ac.id

Article Info

Article info:
Received: 10-01-2025
Revised: 25-05-2025
Accepted: 27-05-2025

Keywords:
Tsunami impact; agricultural soil; resistivity method; soil pH; Wenner configuration

How To Cite:
A. Rahiel, Amsir, Z. Masrurah, Marwan, and M. A. Mohammed, "Analysis of Agricultural Soil Conditions 20 Years Post-Tsunami Using Resistivity and Soil pH Methods", Indonesian Physical Review, vol. 8, no. 2, p 569-585, 2025.

DOI:
https://doi.org/10.29303/ipr.v8i2.463.

Abstract

The tsunami that struck Aceh in 2004 caused significant damage to agricultural land, altering soil properties and affecting productivity. Mon Ikeun Village was one of the most affected areas in the Lhoknga Subdistrict of Aceh Besar Regency. As an agricultural area vulnerable to soil salinization, it faced reduced soil quality, fertility, and nutrient availability risks, which could significantly decrease crop productivity. Therefore, assessing the current condition of agricultural soils is essential to determine whether recovery has occurred or if contamination persists. This research investigates the condition of agricultural soils two decades after the tsunami by analyzing resistivity and soil pH measurements. The resistivity data were collected using a SuperSting R8 device with a Wenner configuration and subsequently processed with IPI2WIN. The pH was determined with a Hanna HI 991001 pH Meter. The results reveal that the affected soils present resistivity values between 9.06 Ωm and 131 Ωm, indicating compositions of sandy clay and sand layers. Soil pH ranges from 4.9 to 6.2, indicating slightly acidic to near-neutral conditions, suitable for agriculture. These results indicate a substantial recovery in soil conditions, especially when compared to a control site in a non-affected area with similar land characteristics. This reinforces the interpretation that the tsunami's impact has diminished over time. This recovery is likely influenced by natural processes such as leaching of contaminants through rainfall. This integrated approach effectively evaluates long-term changes in agricultural soil affected by the tsunami. However, to obtain a clearer understanding of the soil recovery process, future studies could include additional measurements such as soil nutrient analysis, electrical conductivity, or salinity levels to offer more detailed insights.

Introduction

Natural disasters such as tsunamis can cause severe damage to infrastructure and ecosystems, including farmland. The tsunami that struck Aceh on December 24, 2004, significantly affected agricultural regions, leading to a decline in soil quality and productivity, which are vital for supporting the livelihoods of the local community [1]. This phenomenon is attributed to seawater intrusion and sediment deposits brought in by tsunami waves, which alter soil structure and composition, affecting fertility. Tsunamis can significantly change the characteristics and quality of soil by transporting various pollutants, such as heavy metals and hazardous chemicals, thus leading to soil contamination and posing risks to human health and the sustainability of ecosystems [2], [3]. In addition, tsunamis can change the soil's physicochemical characteristics, including pH levels and electrical conductivity, directly impacting soil fertility. A study in the coastal regions of Palu revealed that tsunami sediments have a mineral composition akin to native soils but typically show increased salinity levels, limiting nutrient availability for vegetation and degrading soil quality [4]. One of the regions notably impacted by the 2004 tsunami is Lhoknga Subdistrict in Aceh Besar Regency. This region, mainly composed of agricultural areas, is likely to experience severe soil salinization that compromises the soil and adversely impacts its fertility and the availability of essential plant nutrients. These effects can significantly contribute to a decline in agricultural productivity, directly influencing soil fertility and the availability of critical crop nutrients, leading to decreased agricultural productivity. Consequently, it is crucial to evaluate the post-tsunami condition of agricultural soils to determine whether these soils have fully recovered or remain impaired.

Resistivity methods can be employed to analyze soil characteristics and assess the changes in agricultural soil conditions post-tsunami contamination. At the same time, pH measurements are essential for evaluating the effects of contamination on soil fertility and crop yield. The resistivity method entails injecting electrical currents into the soil and measuring the corresponding resistivity values [5]. This approach is particularly beneficial for identifying subsurface soil structures and characteristics. It is also non-invasive, reducing environmental impact during assessments, and is economically viable [6]. The resistivity method has been effectively used to study soil layer structures in peatlands. For example, a study identified the depth, thickness, and variations in resistivity of soil layers utilizing this method [7]. Moreover, this approach can be integrated with pH measurements due to the correlation between soil pH and electrical resistivity values [8]. Another study using the resistivity method combined with soil pH analysis demonstrated significant efficacy in assessing soil fertility. The results indicated that soil acidity levels impact fertility and can be used to evaluate soil characteristics based on the resistivity values acquired [9]. Furthermore, an additional study supporting these findings shows that combining both methods yields reliable results. The research found that resistivity values typically increase as soil acidity (pH) levels fall [10].

This integrated approach provides a comprehensive strategy for evaluating soil conditions and determining the extent of recovery from tsunami contamination. In addition to evaluating soil resistivity and pH to assess fertility, this study also examined whether agricultural soils in the region remained contaminated or had reverted to their normal state. The choice of control and affected areas in this research was determined by their level of tsunami exposure and similarities in land use for agriculture. Mon Ikeun Village in Lhoknga District was chosen as the affected area due to its coastal position and the severe damage it experienced from the 2004 tsunami, which led to a potential for considerable changes in the physical and chemical characteristics of the soil, negatively impacting the agricultural fertility of the area. Lambaed Village in Kuta Baro District was not affected by the tsunami and was selected as a control site to evaluate soil recovery more accurately. The similarity of characteristics of agricultural land enhances the accuracy of the comparison and elucidates the soil recovery process in coastal regions impacted by the tsunami.

Regional Geology

The investigation occurred in Mon Ikeun Village, in the Lhoknga Subdistrict of Aceh Besar Regency. This study area features various geological formations, such as the Lhoknga Formation (Mul), Peunasu Formation (Tlp), Reef Member Formation (Murl), and undifferentiated Alluvium Formation (Qh), as depicted in Figure 1. The dominant composition of Lhoknga Subdistrict is the Lhoknga Formation (Mul), which is made up of dark-hued, laminated marl limestones that were formed during the Jurassic to Cretaceous epochs [11]. These marl limestones belong to the Woyla Group, which includes rocks created during the late Jurassic to Cretaceous periods and stretches alongside the Barisan Mountain Range from Aceh to West Sumatra [12]. The rocks found within the Woyla Group are noted for their oceanic origins and are significantly affected by faulting, fracturing, and folding; segments of this group signify accretionary rocks that resulted from subduction activities. Moreover, some of the rocks in the Woyla Group are thought to have come from the Sikuleh microcontinent, which developed along the northern boundary of the Gondwana supercontinent and later migrated to collide with Sundaland or the Eurasian Plate [13].

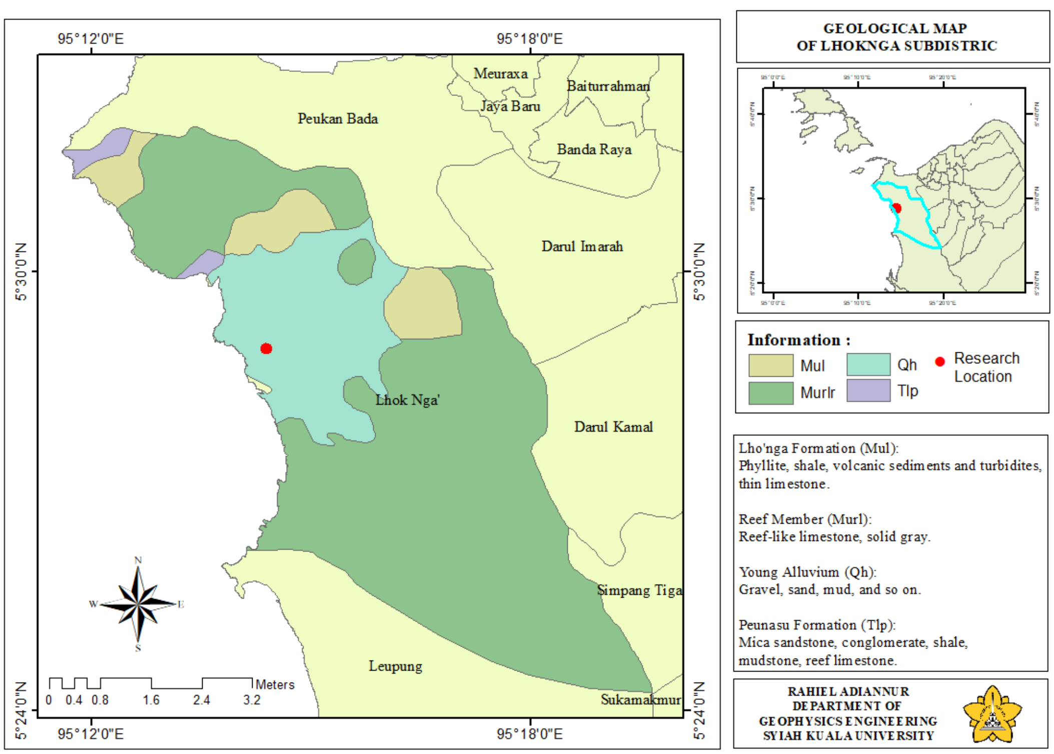

Figure 1. Geological map of Lhoknga Subdistrict

Theory and Calculation

The resistivity method is a geophysical approach employed to examine subsurface conditions by leveraging the electrical characteristics of rocks. This technique introduces high-voltage direct current (DC) into the ground [14]. The core principle behind this measurement involves sending electrical current through two current electrodes (labelled as "C") and evaluating the potential difference response via two potential electrodes (marked as "P"), as depicted in Figure 2. The arrangement of these four electrodes adheres to the chosen electrode configuration, where the distance between electrodes dictates the depth of the subsurface layer. The measurements obtained through this method rely on Ohm's Law, which systematically connects the electrical current flowing through a medium to the induced potential difference [15]. In mathematical terms, Ohm's Law can be represented as shown in equation (1).

$$\Delta V = IR \tag{1}$$

In practical scenarios, the Earth is a heterogeneous medium with differing resistivity values across various layers [16]. Due to these resistivity fluctuations and variations in medium thickness, the recorded resistivity is known as apparent resistivity, which is consistently expressed by equation (2).

$$\rho_a = K\frac{\Delta V}{I} \tag{2}$$

Where K signifies the geometric factor influenced by the electrode layout or configuration utilized during the measurement.

The resistivity of a rock signifies its capacity to hinder the passage of electrical current. Different rock types present a specific range of resistivity values influenced by water content, porosity, density, and permeability [17]. As illustrated in Table 1, the range of resistivity values can aid in distinguishing rock types by considering the regional geological conditions.

Table 1. Electrical resistivity values for different materials [5].

No	Material	Resistivity (Ωm)
1	Sand	1 - 1.000
2	Clay	1 – 100
3	Sandy Clay/Clayey Sand	30 – 215
4	Alluvium	10 – 80

During data collection using this setup, the electrodes are simultaneously moved outward, with the electrode spacing (a) kept constant. The Wenner configuration presents benefits, such as enhanced precision in potential readings at the potential electrodes (P_1 and P_2) owing to their proximity to the current electrodes (C_1 and C_2). Additionally, this setup is susceptible to lateral variations, rendering it suitable for investigations aimed at shallow depths. The arrangement of electrodes in the Wenner configuration is depicted in Figure 2.

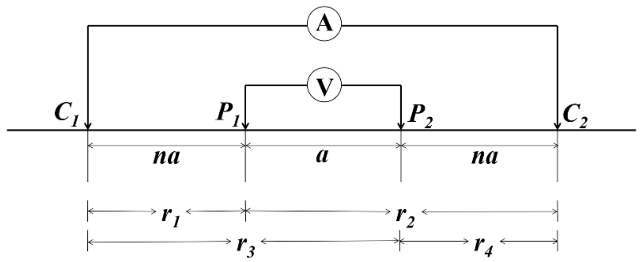

Figure 2. The arrangement of electrodes in the Wenner configuration

The configuration of the electrodes influences the geometric factor (K), which in the Wenner configuration can be calculated using the subsequent formula, as shown in equation (3).

$$K = 2\pi a \tag{3}$$

Experimental Method

Data were collected from two sites used as agricultural land, specifically in rice fields and farms that used to plant coconut, papaya, or banana. Mon Ikeun Village in the Lhoknga Subdistrict of Aceh Besar Regency served as the impacted site by the tsunami, and Lambaed Village in the Kuta Baro Subdistrict of Aceh Besar Regency served as the control site. Mon Ikeun Village in Lhoknga District was selected as the affected area due to its coastal position and severe devastation from the 2004 tsunami. In contrast, the control area was identified in Lambaed Village, Kuta Baro District, a region not impacted by the tsunami, serving as a benchmark for evaluating soil recovery. Both locations share characteristics as agricultural regions, facilitating a more precise comparison. The data collection occurred in December 2024 using a Supersting R8 instrument configured in the Wenner arrangement. This configuration is used because it exhibits a notable sensitivity to vertical variations in subsurface resistivity directly beneath the array's center [16]. The short distance between electrodes allows for more precise data acquisition for shallow depth targets. Additionally, the ease of moving the electrodes accelerates the acquisition process, leading to more effective data collection [18]. Measurements in the tsunami-affected area were taken at four survey points, while the control area included two survey points. Each survey point's traversal length is 2.4 meters, as depicted in Figure 3. The measurement path length was chosen to gather more precise data for shallow areas, as the tsunami deposits are usually found at 0 to 1 meter [19].

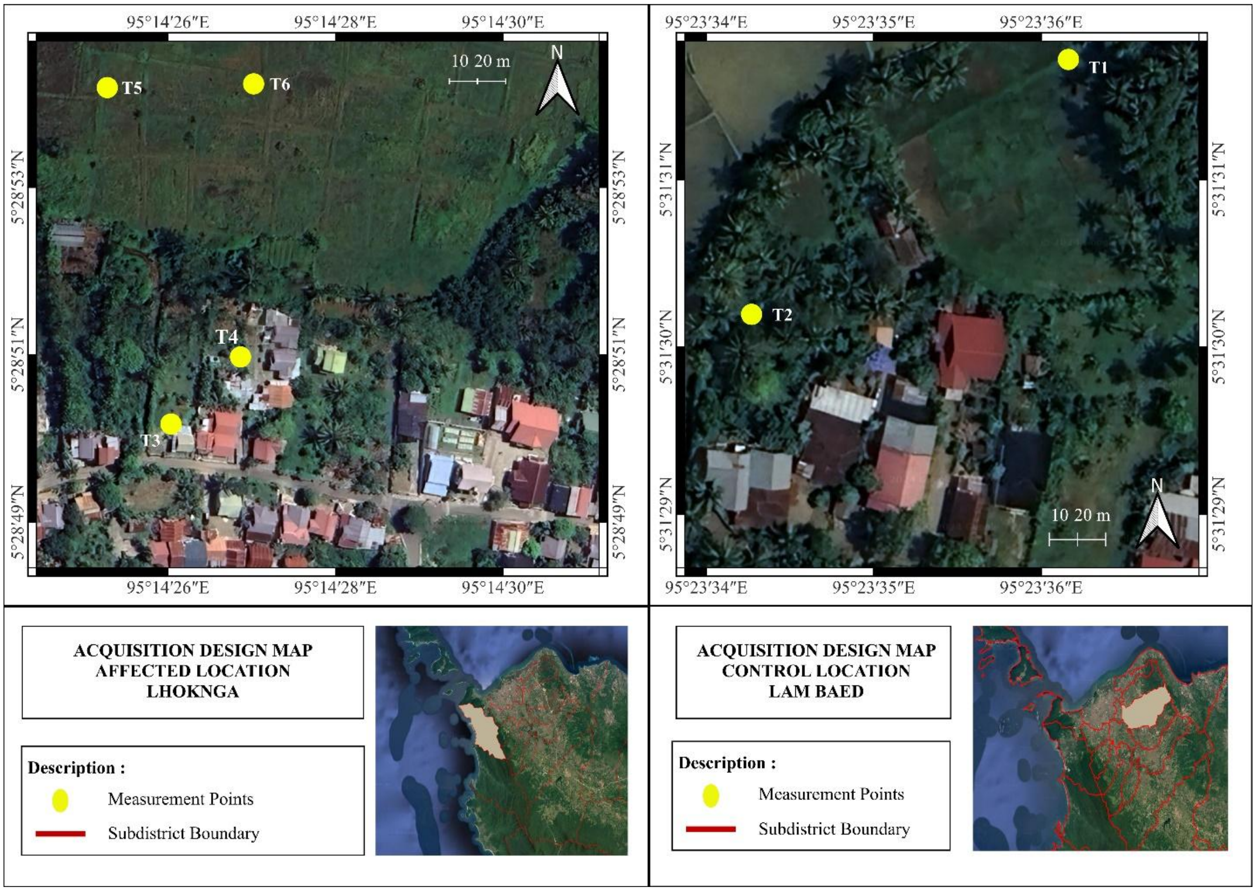

Figure 3. Acquisition map of the research area

Soil pH assessments were conducted at each survey point in both locations using a Hanna Instrument HI 991001 pH Meter. Data collection was performed under sunny weather. The data collection process involves creating a hole that is 0.5 meters deep. The pH electrode is rinsed with distilled water and wiped to restore the tool to a neutral state. The pH meter is then calibrated to confirm that the instrument is ready for use in a neutral condition. Measurements of soil pH are conducted by placing the electrode directly into the soil, allowing it to remain there for 1 to 2 minutes to achieve stable readings, and this process is repeated three times in each measurement point. The pH value obtained from field measurements is then recorded in a data table and analyzed using suitable data techniques to evaluate the chemical properties of the soil and determine its suitability for agricultural use. However, pH measurements in the affected location of the ricefield could not be acquired beyond a depth of 0.24 m because rain several days prior had caused water to seep in from the ground. The resistivity data were analyzed with IPI2WIN software through an inversion procedure, converting apparent resistivity data into true resistivity values. The output from this process generated a subsurface model that displayed resistivity values, depths, and the thicknesses of each layer. Data analysis is based on the resistivity values listed in Table 1 and refers to the regional geological conditions of the research location. The soil pH data were processed to obtain the mean values and to construct a graphical representation, which was subsequently utilized to evaluate the soil acidity levels at the study locations.

Result and Discussion

Six data points were collected during the acquisition using the Wenner configuration, T1 through T6. The length of each track was set to 0.8 m to obtain a good penetration with shallow depths—figures 4 and 5 show resistivity curves derived from the inversion processes. The depth achieved for each layer extends up to 40 cm, with differing layer thicknesses. In Figure 4, the resistivity values span from 2.01 to 22.5 Ωm, as shown in Table 2, with depths reaching up to 0.4 m. Due to the relatively minor variation in resistivity values, it is inferred that the subsurface material at this measurement point is predominantly clay. In contrast, Figure 5 presents resistivity values from 2.33 to 26.64 Ωm, shown in Table 3, attaining a maximum depth of 0.5 m. The resistivity variation at T2 remains similar to that recorded at T1, concluding that the subsurface material is likely clay.

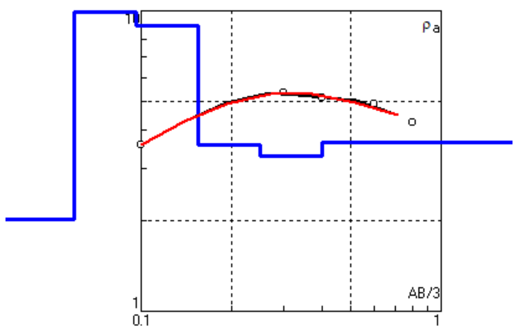

Figure 4. Inversion results for T1 at the control location. The white dots and the black line represent the recorded data (observer curve), the red line illustrates the mathematical model designed to predict the expected response in the subsurface (synthetic curve). In contrast, the blue line indicates the number of layers below the surface.

Table 2. Resistivity values on T1 at the control location.

No	Resistivity Values (Ωm)	Height (m)	Depth (m)
1	2.01	0.06	0.06
2	22.5	0.036	0.10
3	8.92	0.059	0.16
4	3.57	0.094	0.25
5	3.27	0.151	0.4
6	3.66		

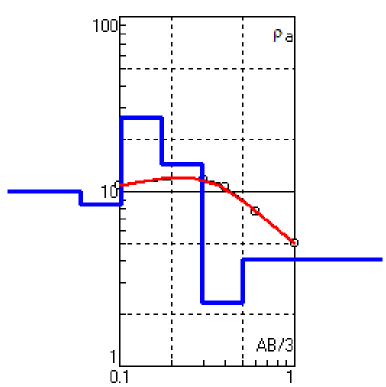

Figure 5. Inversion results for T2 at the control site.

Table 3. Resistivity values on T2 at the control location.

No	Resistivity Values (Ωm)	Height (m)	Depth (m)
1	9.94	0.06	0.06
2	8.37	0.042	0.10
3	26.64	0.071	0.17
4	14.32	0.121	0.29
5	2.33	0.206	0.5
6	4.11		

Measurement Point T3 in the area impacted by the tsunami is depicted in Figure 6. The variation in resistivity values is shown in Table 4, ranging from 9.06 Ωm to 118.1 Ωm. The maximum depth recorded at this point is 0.4 m, with different thicknesses of layers. Considering the observed range of resistivity, it is hypothesized that the subsurface materials at this location are mainly composed of sand.

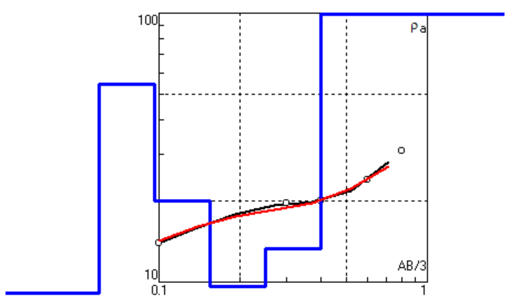

Figure 6. Inversion results for T3 at the tsunami-affected location.

Table 4. Resistivity values on T3 at the tsunami-affected location.

No	Resistivity Values (Ωm)	Height (m)	Depth (m)
1	9.06	0.06	0.06
2	54.37	0.036	0.10
3	19.99	0.059	0.16
4	9.61	0.094	0.25
5	13.25	0.151	0.4
6	118.1		

On the other hand, T4 in the impacted area is thought to have different subsurface materials compared to T3. The inversion outcomes for T4 are depicted in Figure 7, where the resistivity measurements at this location vary between 30.94 Ωm and 99.86 Ωm, as presented in Table 5, suggesting that the subsurface material is probably sandy clay.

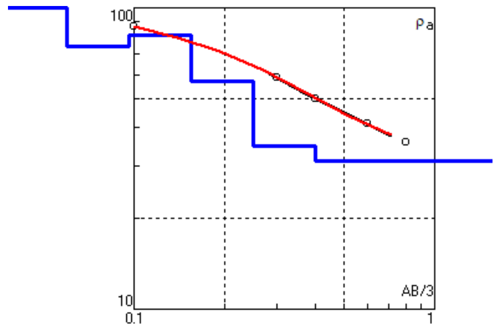

Figure 7. Inversion results for T4 at the tsunami-affected location.

Table 5. Resistivity values on T4 at the affected location

No	Resistivity Values (Ωm)	Height (m)	Depth (m)
1	99.86	0.06	0.06
2	74.25	0.036	0.10
3	80.98	0.059	0.16
4	57.3	0.094	0.25
5	34.73	0.151	0.4
6	30.94		

The changes in resistivity values at T5 within the affected zone are illustrated in Figure 8. Table 6 shows that resistivity values vary between 38.88 Ωm and 128.7 Ωm, extending to a depth of 0.4 m with different thicknesses. Layers 1 to 3, which span from a depth of 0 to 0.15 m and show resistivity values from 53.92 Ωm to 128.7 Ωm, can be interpreted as sand. In contrast, the layer that stretches from a depth of 0.16 m to 0.4 m, with resistivity values from 38.88 Ωm to 53.96 Ωm, is likely composed of clay material.

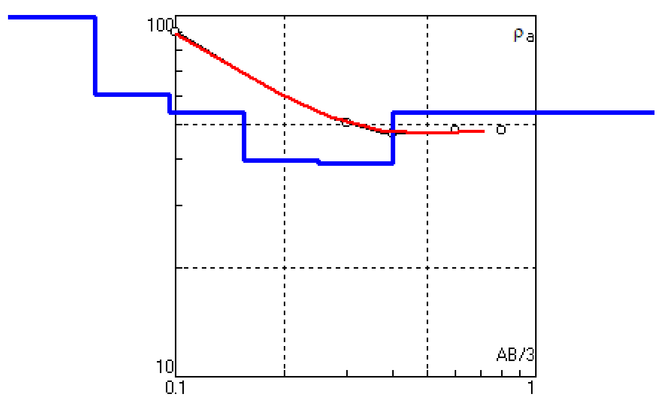

Figure 8. Inversion results for T5 at the tsunami-affected location.

Table 6. Resistivity values on T5 at the tsunami-affected location.

No	Resistivity Values (Ωm)	Height (m)	Depth (m)
1	128.7	0.06	0.06
2	60.39	0.036	0.10
3	53.92	0.059	0.16
4	39.72	0.094	0.25
5	38.88	0.151	0.4
6	53.96		

The resistivity values recorded at T6 in the affected area are indicated in Figure 9. Based on Table 7, these values range from 13.12 Ωm to 57.42 Ωm, suggesting that this layer consists of alluvium. The deepest measurement at this point reaches 0.4 m, with each layer displaying unique thicknesses.

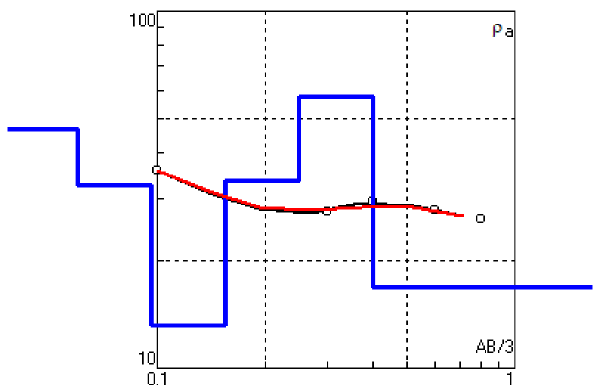

Figure 9. Inversion results for T6 at the tsunami-affected location.

Table 7. Resistivity values on T6 at the tsunami-affected location.

No	Resistivity Values (Ωm)	Height (m)	Depth (m)
1	46.68	0.06	0.06
2	32.69	0.036	0.10
3	13.12	0.059	0.16
4	33.58	0.094	0.25
5	57.42	0.151	0.4
6	16.87		

Resistivity and salinity values have an inverse correlation, also known as negative linear correlation, where the salinity value will decrease if there is an increase in resistivity values [20]. In the land recovery process after the tsunami, a gradual rise in resistivity over time can indicate that the salt content previously deposited due to the tsunami has decreased. On the other hand, the low resistivity measurement at the control site, which was not impacted by the tsunami, is believed to be affected by weather factors, particularly rainfall that happened a day before data collection. It is known that the control site consists of clay, a material known for its low water permeability, which is one of the elements thought to play a role in the low resistivity observed there [21]. Given that the pH of the soil is within the neutral range at the study site, it can be inferred that the agricultural land currently possesses a favorable level of fertility. The thriving growth of rice, corn, and papaya crops in the research area further evidences this.

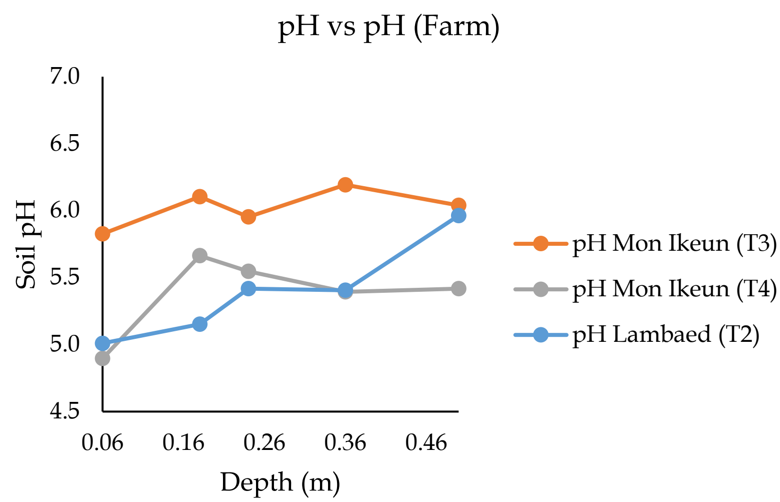

Figure 10. Depth curve against pH in the farm

According to Figure 10, which shows the pH values at different depths, it can be seen that the pH levels at the impacted site are only slightly different from those at the control site. The acidity in the agricultural land of the affected region varies between 4.9 and 6.2, suggesting that the soil is somewhat acidic to nearly neutral, with soil types predominantly consisting of sand and sandy clay [22]. This indicates that the land is relatively fertile for farming, as demonstrated by the successful cultivation of several crops, including papaya, banana, and coconut, which can grow in a pH range from a minimum of 6 to a maximum of 7.5 [23]. Figure 10 shows that T3 has a pH level closer to neutral than T4, and both of these measurement points are on the affected sites.

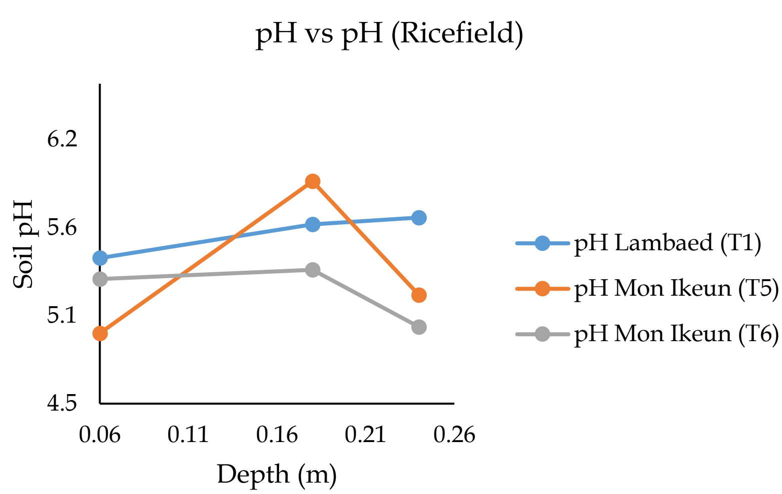

Figure 11. Depth curve against pH in the rice field

The soil acidity levels measured at the impacted site (T5 and T6) ranged from 4.9 to 5.9, signifying that the soil in this region can be classified as slightly acidic, akin to the soil conditions in the earlier farm area [22]. Both areas are in the same geological formation, specifically Qh (Younger Alluvium), thus showing similar geological characteristics. The similarity of geological conditions provides a consistent basis for comparison, so that differences in soil properties between the two can be attributed more to external factors, such as the impact of the tsunami [11]. The pH levels recorded also lie within the suitable range for rice production (5 to 6.5) and a variety of other crops like corn (which can grow in a pH range of 5.5 to 7), implying that the soil in this region is nutrient-rich, indicating that this area can be described as fertile [23]. As illustrated in Figure 11, the variations in soil acidity between the affected areas and the control sites are minimal. However, the soil pH at depths of 0.36 m and 0.5 m could not be assessed due to water intrusion during the excavation process, resulting in pH values of zero at those depths. From this data, it can be inferred that tsunami contamination has lessened across the four measurement points in the designated tsunami-affected area.

Research carried out in the Aceh Besar District, specifically in the villages of Tibang and Kajhu, revealed that the resistivity values of tsunami deposits for clay materials ranged from 0.53 to 0.9 Ωm, while for sand materials, it was in the range of 2 to 3.42 Ωm [19]. In contrast, the resistivity measurements taken in Mon Ikeun Village, Lhoknga District's impacted area, varied from 9.06 to 128.7 Ωm, predominantly sand and sandy clay. This difference indicates that agricultural land at the research site no longer exhibits the resistivity characteristics of tsunami deposits. This leads to the conclusion that the soil in the area has recovered and is no longer contaminated. Compared to earlier research, the soil pH value in the tsunami-impacted region of Nagapattinam District, India, ranged from 7 to 8.4, indicating alkaline conditions. In contrast, in the South Andaman area, it ranged from 4.7 to 7.2, reflecting soil with acidic to neutral characteristics [24], [25]. In contrast, the findings of this study reveal that the soil pH at the location examined falls between 4.9 and 6.2, positioning it between the two previous studies and representing slightly acidic to nearly neutral conditions. This result suggests that the soil at the study site exhibits a relatively neutral state, which can indicate the recovery process in post-tsunami agricultural land. Furthermore, contamination may gradually lessen or vanish due to natural methods such as rainfall or leaching [24]. Rainwater is particularly effective in dissolving and removing salts from agricultural soils, restoring soil acidity to its natural condition [25].

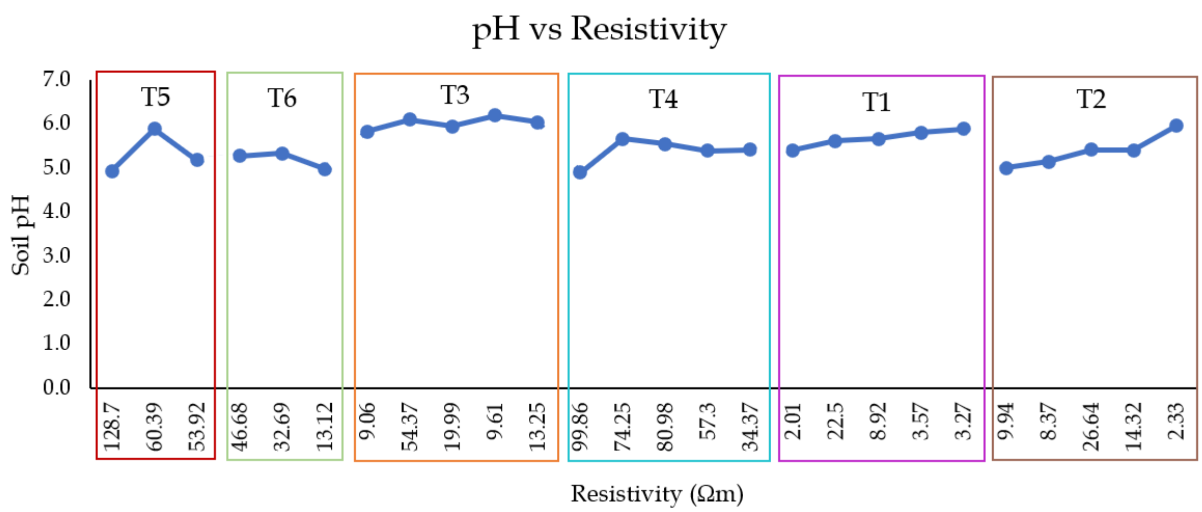

Figure 12. Resistivity curve against pH at all measurement points

The soil resistivity and pH data obtained at each measurement point are illustrated in Figure 12. From a total of 24 data collection points, six were selected for further analysis based on the completeness of resistivity and pH data, as they were representative of the site's soil conditions. Based on Figure 12, points T1 and T2 show low resistivity, indicating clay soil ranging from 2.01 to 26.64 Ωm. The low resistivity value is not caused by tsunami contamination, as this site is unaffected by the tsunami, and rain on the day before the measurement resulted in damp soil, leading to a transient reduction in soil resistivity. This aligns with findings from the ITERA arboretum area, where a low resistivity value was recorded alongside a high soil pH, which was influenced by weather conditions [5], [8]. The pH value of the soil at the control location is slightly acidic to nearly neutral, ranging from 5.0 to 6.0. This condition remains within the ideal pH levels for commonly grown crops in the region, including rice (5.0–6.5) and coconut (6.0–7.5), making this area indeed suitable for agricultural use [23], [26]. At point T3, the resistivity measurements vary between 9.06 and 118.1 Ωm, which suggests the presence of moist sandy soil. The pH value, ranging from 5.8 to 6.2, indicates nearly neutral soil conditions. This condition reflects that the tsunami no longer contaminates the soil at this measurement point. Furthermore, the healthy growth of plants like papaya in the area further supports the notion that the soil at this location is in good condition for agricultural cultivation [5], [26].

The range of resistivity values on T4 is from 34.37 to 99.86 Ωm, suggesting that the soil is classified as sandy clay. The pH value of 4.9 to 5.7 indicates that the soil is notably acidic. However, the presence of water apple plants that grow well in this area implies that the land remains viable for cultivating other plants that can tolerate similar pH levels, given that water apples thrive optimally within a pH range of 5.5 to 7.5 [5], [26], [27]. PH corrections are required to enhance the growth of plants that prefer more neutral pH conditions. The resistivity value at point T5 ranges from 53.92 to 128.7 Ωm, with a soil pH value between 4.9 and 5.9. Based on these data, the soil type at this location is interpreted as sand and clay with slightly acidic conditions. Nevertheless, the pH levels remain suitable for growing food crops like rice, which thrives at a pH of 5.0 to 6.5, and corn, which prefers a pH of 5.5 to 7.0 [5], [23],

[26]. Therefore, this area is considered a relatively optimal choice for agricultural purposes, particularly for crops that can tolerate slightly acidic soil conditions.

According to Figure 12, the soil at location T6 has a resistivity range of 13.12–46.68 Ωm and a pH between 5.0 and 5.3, indicating an alluvial soil type with moderately acidic conditions. The pH remains within the ideal range for rice cultivation, although it is less suitable for corn, which requires a more neutral pH [5], [23], [26]. The resistivity value at T6 is also relatively high and does not indicate a significant decrease that usually occurs due to tsunami contamination. This suggests that the soil in this area is still in relatively good condition and is no longer contaminated by the tsunami. However, for corn cultivation, or corn cultivation, pH adjustment and proper nutrient management are necessary to support optimal growth. Based on the graph shown in Figure 12, the findings regarding the link between resistivity values and soil pH reveal a trend of an inverse relationship, where higher resistivity values are typically accompanied by lower pH values, and vice versa [28]. The resistivity and pH values obtained at the study sites indicate that the land remains suitable for agricultural use and does not exhibit strong indications of contamination due to the tsunami.

Conclusion

The agricultural land in the study area is predominantly composed of clay and sandy soils, with resistivity values ranging from 2.01 to 131 Ωm as determined through inversion. Based on field measurements, the pH values of the soil range from 4.9 to 6.2, indicating that the soil condition in the agricultural land has returned to its original state. The collected data suggest that the correlation between resistivity and soil pH is negative but weak. This is demonstrated by changes in resistivity values that do not consistently correspond with significant changes in pH. Therefore, further research must thoroughly assess the linear relationship between resistivity and soil pH, considering other relevant variables. Compared to earlier research, this connection aligns with previous findings, where the stabilization of soil pH, accompanied by a high resistivity value, implies that the effects of salinity have reduced in this area. This may be attributed to high rainfall, facilitating dissolved salts' leaching and restoring the soil pH to its original state. In addition, the resistivity values measured in the study area show significantly higher values than the resistivity range of tsunami deposits (0.53 to 3.42 Ωm). This difference strengthens the indication that agricultural land in the study area has recovered from the impact of tsunami contamination. Although the obtained data indicate signs of recovery, further studies, such as geochemical data, are still needed to validate these findings and to ensure a more comprehensive understanding of the long-term soil restoration process in tsunami-affected areas.

Acknowledgment

We sincerely thank all those who contributed to this research, which was fully supported by the MBKM USK Unggul research program. Special appreciation goes to our supervisors for their invaluable assistance throughout the data processing and interpretation stages. Additionally, we genuinely appreciate our colleagues from the Department of Geophysics Engineering at Universitas Syiah Kuala for their help during the data collection phase. Finally, we sincerely thank the residents of Mon Ikeun Village in Lhoknga Subdistrict and Lambaed

Village in Kuta Baro Subdistrict, both situated in Aceh Besar Regency, Aceh Province, for their warm welcome and generous cooperation throughout this study.

References

[1] Universitas Syiah Kuala, 'Peneliti USK dan Unsam : Sedimen Tsunami Berpengaruh pada Tumbuhan Kebun', 2022. [Online]. Available: https://usk.ac.id/peneliti-usk-dan-unsam-sedimen-tsunami-berpengaruh-pada-tumbuhan-kebun/. [Accessed: April. 28, 2025].

[2] T. Yamaguchi, T. Sato, M. Katoh, " Post-depositional changes in elemental leaching from recovered soils separated from disaster waste and tsunami deposits generated by the Great East Japan Earthquake and tsunami," *Journal of Environmental Management*, vol. 233, pp. 89-96, 2019.

[3] Y. Kawabe, J. Hara, T. Yasutake, Y. Sakamoto, M. Zhang, T. Komai, "Heavy Metal in tsunami sediment by the Great East Japan Earthquake and their risk to human," *J.JSCE Ser. G (Environ. Res.)*, vol. 68, no. 3, pp. 195-202, 2012.

[4] M. Anda, S. Purwanto, E. Suryani, Husnain, Muchtar, "Pristine soil property and mineralogy as the strategic rehabilitation basis in post-earthquake-induced liquefaction, tsunami and landslide in Palu," *Catena*, vol. 203, no. 105345, pp. 1-16, 2021.

[5] W. Telford, L. Geldart, R. Sheriff, "Applied Geophysics," *Cambridge University Press*, 1990.

[6] O. Sanuade, K. Arowoogun, J. Amosun, "A review on the use of geoelectrical methods for characterization and monitoring of contaminant plumes," *Acta Geophysica*, vol. 70, no. 5, pp. 2099-2117, 2022.

[7] E. Sapina, L. Handayani, J. Pebralia, "Identifikasi Struktur Lapisan Tanah Pada Lahan Gambut Dengan Metode Resistivitas Konfigurasi Wenner-Schlumberger," *Jurnal Geofisika Eksplorasi*, vol. 9 no. 2, pp. 142-149, 2023.

[8] A. Nabilla, M. Alimuddin, Y.A. Paembonan, "Analisis Perbedaan Data Resistivitas Terhadap Data Kimia dan Fisika Tanah Terhadap Kondisi Tanah Daerah Arboterum ITERA," *Jurnal Geofisika Eksplorasi*, pp. 1-14, 2021.

[9] M. Kahfi, F.P. Ahmad, "Klasifikasi Kesuburan Tanah Menggunakan Parameter Resistivitas, Kadar Air, dan pH Tanah Studi Kasus : Tanaman Jagung," *Jurnal Fisika Unand*, vol. 12 no. 2, pp. 193-199, 2023.

[10] D. Bravo, J. Benavides-Erazo, "The use of two-dimensional electrical resistivity tomography (2D-ERT) as a technique for cadmium determination in Cacao crop soils," *Applied Sciences*, vol. 10, pp. 1-16, 2020.

[11] J.D. Bennet, from Geologic Map of the Banda Aceh Quadrangle, 1981.

[12] A.J. Barber, M.J. Crow, J.S. Milsom, "Sumatra, Geology, Resources, and Tectonic Evolution," *Geological Society London*, 2005.

[13] A.J. Barber, "The Origin of The Woyla Terranes in Sumatra and The Late Mesozoic Evolution of the Sundaland Margin," *Journal og Asian Earth Sciences*, vol. 18, no. 6, pp. 713-738, 2000.

[14] A. Ashari, M. Iryanti, A. Aminudin, "Analisis Nilai Resistivitas Struktur Lapisan Bawah Permukaan Tanah Menggunakan Metode Geolistrik Konfigurasi Wenner-Schlumberger Di Desa Rancakole Kabupaten Bandung," *Seminar Nasional Fisika 5.0.*, vol. 1 no. 1, pp. 279-287, 2019.

[15] J.M. Reynolds, "Electrical Resistivity Methods," *in An Introduction to Applied and Environmental Geophysics,* Country: United Kingdom, 2011, ch. *7*, sec. *7.2.1*, pp. *289-292*.

[16] Loke M., "Tutorial :2-D and 3-D electrical imaging surveys," 2023.

[17] B. Septyanto, M. Nafian, N. Isnaini, "Identifikasi Lapisan batuan di Daerah Bojongsari Depok Menggunakan Metode Resistivitas Menggunakan Metode Geolistrik Resistivitas," *Al-Fiziya*, vol. 1 no. 2, pp. 1-8, 2018.

[18] A. Riadi, M. Lenny, K.D. Ira, "Identifikasi Zona Lemah dengan Metode Geolistrik Konfigurasi Wenner di Kelurahan Terusan Kecamatan Maro Sebo Ilir Kabupaten Batanghari," *JoP*, vol. 9 no. 2, pp. 6-11, 2016.

[19] M. Syukri, S. Rosli, T.A. Sabrian, F. Zul, "Resistivity and Chargeability Signatures of Tsunami Deposits at Aceh Besar and Banda Aceh Coastal Area, Indonesia," *Geomate*, vol.17, no. 59, pp. -133-143, 2019.

[20] Khairunnas, G. Mulya, "Analisis Pengaruh Parameter Konduktivitas, Resistivitas dan TDS Terhadap Salinitas Air Tanah Dangkal pada Kondisi Air Laut Pasang dan Air Laut Surut di Daerah Pesisir Pantai Kota Padang," *Jurnal Bina Tambang*, vol. 3 no. 4, pp 1751-1760, 2018.

[21] H. Julkrisman, G. Murniwati, "Analisis Permeabilitas Tanah Berpasir dan Tanah Lempung dalam Hubungannya dengan Manajemen Irigasi," *PENARIK: Jurnal Ilmu Pertanian dan Perikanan*, vol. 1 no. 2, pp. 60-67, 2024.

[22] Dinas Pertanian dan Pangan Kota Sabang, 'Pentingnya Pengukuran pH Tanah', 2022. [Online]. Available: https://distanpangan-dev.sabangkota.go.id/berita/kategori/pendidikan-pelatihan/pengukuran-ph-tanah-di-jaboi. [Accessed: Oct. 11, 2024].

[23] Dinas Pertanian Kabupaten Mesuji, 'Pentingnya Memahami pH Tanah', 2021. [Online]. Available: https://pertanian-mesuji.id/pentingnya-memahami-ph-tanah/. [Accessed: April. 28, 2024].

[24] T. Kume, C. Umetsu, K. Palanisami, "Impact of the December 2004 tsunami on soil, groundwater and vegetation in the Nagapattinam district, India," *Journal of Environmental Management*, vol. 90, pp. 3147-3154, 2009.

[25] A. Velmurugan, T. Swarnam, R. Lal, "Effect of land shaping on soil properties and crop yield in tsunami inundated coastal soils of Southern Andaman Island," *Agriculture, Ecosystems and Environment*, vol. 206, pp. 1-9, 2015.

[26] P.K. Abdi, N.H. Rini, S.D. Harry, "DSS untuk Menganalisis pH Kesuburan Tanah Menggunakan Metode *Single Linkage*," *EECCIS,* vol. 8 no. 1, pp. 1-9, 2014.

[27] L. Firman, L. Naila, S.H. Ariani, "Tanaman Jambu Air Madu," *in Ekoenzim dan Pengaruhnya Terhadap Pertumbuhan Stek Jambu Air Madu Deli Hijau (Syzygium aqueum)*, Country: Sukoharjo, 2023, ch. *1*, sec. *1.2*, pp. *8*.

[28] S. Ina, W. Iwa, IGN. Janardana, "Pengaruh Potensial Hidrogen (pH) Tanah terhadap Tahanan Jenis Tanah untuk Mendapatkan Bentuk Sistem Pembumian," *Jurnal Spektrum,* vol. 6 no. 4, pp. 29-35, 2019.